

## HST NICMOS IMAGING OF THE PLANETARY-MASS COMPANION TO THE YOUNG BROWN DWARF 2MASSW J1207334–393254

INSEOK SONG,<sup>1</sup> G. SCHNEIDER,<sup>2</sup> B. ZUCKERMAN,<sup>3</sup> J. FARIHI,<sup>1</sup> E. E. BECKLIN,<sup>3</sup> M. S. BESSELL,<sup>4</sup>  
P. LOWRANCE,<sup>5</sup> AND B. A. MACINTOSH<sup>6</sup>

Received 2005 August 25; accepted 2006 July 20

### ABSTRACT

Multiband (0.9–1.6  $\mu\text{m}$ ) images of the TW Hydrae association (TWA) brown dwarf 2MASSW J1207334–393254 (also known as 2M 1207) and its candidate planetary-mass companion (2M 1207b) were obtained on 2004 August 28 and 2005 April 26 with *HST* NICMOS. The images from these two epochs unequivocally confirm the two objects as a common proper motion pair (16.0  $\sigma$  confidence). A new measurement of the proper motion of 2M 1207 implies a distance to the system of  $59 \pm 7$  pc and a projected separation of  $46 \pm 5$  AU. The NICMOS and previously published VLT photometry of 2M 1207b, extending overall from 0.9 to 3.8  $\mu\text{m}$ , are fully consistent with an object of a few Jupiter masses at the canonical age of a TWA member ( $\sim 8$  Myr) based on evolutionary models of young giant planets. These observations provide information on the physical nature of 2M 1207b and unambiguously establish that the first direct image of a planetary-mass companion in orbit around a self-luminous body, other than our Sun, has been secured.

*Subject headings:* planetary systems — stars: individual (2MASSW J1207334–393254) — stars: low-mass, brown dwarfs

### 1. INTRODUCTION

Beginning in 2004 July, with the *Hubble Space Telescope* (*HST*) Near-Infrared Camera and Multi-Object Spectrometer (NICMOS), we initiated a systematic imaging search for extra-solar gas giant planets around 116 young nearby stars and brown dwarfs. These targets are  $\leq 50$  Myr old and located within 60 pc of Earth, making them among the best-known targets for such a survey (Zuckerman & Song 2004).

A brown dwarf in the  $\sim 8$  Myr old TW Hydrae association, 2MASSW J1207334–393254 (hereafter 2M 1207; Gizis 2002), was included in our *HST* target list, and its observation was planned for 2005 April. However, on 2004 April 27 (UT), 2M 1207 was observed with the Very Large Telescope (VLT) NACO, and a faint companion candidate was discovered  $\sim 0''.78$  from the brown dwarf (Chauvin et al. 2004). NICMOS observations of 2M 1207 were replanned and brought forward to 2004 August. The resulting NICMOS photometric data, shorter in wavelength than could be obtained with adaptive optics on the VLT, support the conjecture that 2M 1207b is of mid to late L type based on its color indices. With the limited precision of the proper-motion data then available for 2M 1207 and the short time between the VLT and 2004 August *HST* observations, common proper motion with 2M 1207b was established at the 2.6  $\sigma$  level (Schneider et al. 2004). Additional observations were obtained with the VLT

during 2005 February and March that much more precisely demonstrated common proper motion between 2M 1207 and its companion (Chauvin et al. 2005a). As described in § 4.1, the proper-motion value of 2M 1207 (Scholz et al. 2005) used in Chauvin et al. (2005a) was not well measured, causing the analysis to be somewhat overoptimistic.

With the higher accuracy *HST* astrometry and a new, more accurate, proper-motion measurement of 2M 1207 in the present paper, we report a more definitive common proper motion between 2M 1207 and 2M 1207b. We also present short near-IR wavelength diagnostic photometry that cannot currently be obtained from the ground given the performance limitations of adaptive optics imaging.

### 2. HST OBSERVATIONS

*HST* near-IR observations of 2M 1207 were obtained with NICMOS camera 1 ( $\sim 43$  mas pixel<sup>-1</sup>) at two observational epochs: 2004 August 28 and 2005 April 26. At each epoch, 2M 1207 was observed at two field orientations (spacecraft roll angles) in successive *HST* orbits to permit self-subtractions of the rotationally invariant point-spread function (PSF), thereby significantly increasing the visibility of the nearby companion. Direct imaging in camera 1, rather than coronagraphy in camera 2, was planned due to the  $\sim 0''.78$  angular separation of 2M 1207 and its putative planetary-mass companion and the relatively benign contrast ratios expected based on the VLT observations. NICMOS camera 1 provides shorter wavelength diagnostic filters than does camera 2 with a commensurately finer pixel scale to permit critical sampling of the PSF at short near-IR wavelengths. Details of the NICMOS observations are listed in Table 1.

Raw MULTIACCUM frames were converted to count-rate images with an IDL-based analog to the STSDAS `caln1ca` task, using calibration reference files developed by the NICMOS Instrument Definition Team and the Space Telescope Science Institute. Known defective pixels (underresponsive due to particulate contamination and those with excessive dark currents) were replaced by two-dimensional Gaussian-weighted interpolations of

<sup>1</sup> Gemini Observatory, Northern Operations Center, 670 North A‘ohoku Place, Hilo, HI 96720; song@gemini.edu, jfarihi@gemini.edu.

<sup>2</sup> Steward Observatory, University of Arizona, 933 North Cherry Avenue, Tucson, AZ 85721; gschneider@as.arizona.edu.

<sup>3</sup> Department of Physics and Astronomy and Center for Astrobiology, University of California, Los Angeles, 475 Portola Plaza, Los Angeles, CA 90095-1547; ben@astro.ucla.edu, becklin@astro.ucla.edu.

<sup>4</sup> Research School of Astronomy and Astrophysics, Institute of Advanced Studies, Australian National University, ACT 2611, Australia; bessell@mso.anu.edu.au.

<sup>5</sup> Spitzer Science Center, Infrared Processing and Analysis Center, MS 220-6, Pasadena, CA 91125; lowrance@ipac.caltech.edu.

<sup>6</sup> I Division, Lawrence Livermore National Laboratory, 7000 East Avenue, Livermore, CA 94550; bmac@igpp.ucllnl.org.

TABLE 1  
NICMOS OBSERVATIONS SUMMARY

UT Date	Orientation Angle <sup>a</sup>	Filters	SAMPSEQ <sup>b</sup>	NSAMP <sup>c</sup>	EXPTIME <sup>d</sup> (s)
2004 Aug 28.....	279°720/289°620	F090M	STEP64	13	2560
	279°720/289°620	F110M	STEP64	12	2048
	279°720/289°620	F160W	STEP8	12	448
2005 Apr 26.....	187°120/207°120	F090M	STEP64	13	2560
	187°120/207°120	F145M	STEP64	12	2048
	187°120/207°120	F160W	STEP8	12	448

<sup>a</sup> Orientation angle of the image positive Y-axis east of north.

<sup>b</sup> MULTIACCUM sample sequence (Noll et al. 2004).

<sup>c</sup> Number of nondestructive readouts for each exposure.

<sup>d</sup> Total exposure time for four filtered images at each orientation for each epoch.

good neighbor pixels (with wavelength-dependent weighting radii of the PSF FWHM for the filters employed). Dark-subtracted, linearity-corrected, flat-fielded, cosmic-ray-rejected count-rate images were postprocessed to remove additional well-characterized detector artifacts. For each filter in each visit, the four images were astrometrically registered to the position of the first image. Position offsets were taken as reported in the downlinked spacecraft telemetry, through the CD matrices in the science data file headers, and verified by Gaussian profile fitting and image centroiding of the 2M 1207 PSF image cores. Image registration was accomplished via sinc function apodized bicubic interpolation, rebinning the interpolated images into a 2 times finer spatially resampled grid. Then images were median combined to create better sampled, higher signal-to-noise ratio (S/N), and defect-minimized count-rate images suitable for PSF subtraction and of high photometric fidelity. Details of the data calibration and processing methodologies are discussed in Schneider et al. (2005).

### 2.1. Photometry

Photometry of 2M 1207b was carried out after reducing the light of the primary star by subtracting the dither-combined image at the second field orientation from the first field orientation. This roll subtraction virtually eliminated the spatially variable light from the primary outside  $0''.2$ , leaving a positive and negative image of 2M 1207b displaced by the differential field rotation. Since the PSFs of the companion partially overlap in this

difference image, model PSFs were created to fit and null out actual image PSFs separately by adjusting position and flux density. This created an image at each orientation with the primary removed and only one companion remaining. These two images of the companion were then rotated by the appropriate spacecraft roll angle and combined (Fig. 1). The model PSFs were created using TinyTim, version 6.1a (Krist & Hook 1997), which produces high-fidelity filter- and position-dependent model PSFs for *HST* instruments.

The in-band flux densities (and Vega system magnitudes) of 2M 1207 were established from the unsubtracted, dither-combined images independently resulting from each orbit. To verify the model PSF subtraction method used to determine the companion magnitudes, we measured the primary magnitudes both with flux-scaled model PSF subtraction and with background-subtracted aperture photometry (corrected to an infinite aperture).

The measured F090M and F160W magnitudes at the two NICMOS epochs are consistent (Table 2), and flux-weighted mean apparent magnitudes from both epoch measurements are  $m_{F090M} = 22.46 \pm 0.25$  mag and  $m_{F160W} = 18.26 \pm 0.02$  mag, respectively.

### 2.2. Astrometry

The NICMOS camera 1 pixel scales applicable to both epochs of our 2M 1207 observations are  $X$ -scale =  $43.190$  mas pixel<sup>-1</sup>,  $Y$ -scale =  $43.016$  mas pixel<sup>-1</sup>. The median combined calibrated

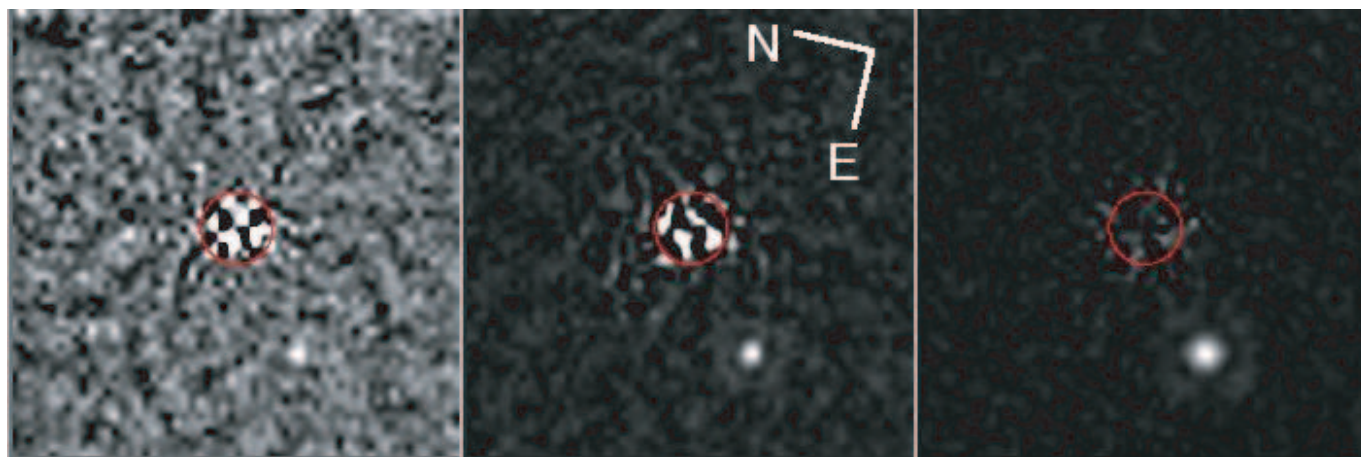


FIG. 1.— First-epoch NICMOS camera 1 PSF-subtracted images of 2M 1207 (centered in the  $0''.2$  radius circle) and its companion ( $0''.77$  to the southeast) at 0.9, 1.1, and  $1.6 \mu\text{m}$  (from left to right). By subtracting a second image of 2M 1207 at a different celestial orientation, background light from the primary at the location of 2M 1207b is effectively eliminated. In addition, in each difference image, a flux-scaled, astrometrically registered model PSF, fit to the “negative” image of 2M 1207b, was added to eliminate the negative imprint from the difference image.

TABLE 2  
PHOTOMETRY OF 2M 1207 AND ITS COMPANION

Name	FILTER 50% Bandpass ( $\mu\text{m}$ )	<i>HST</i> MAGNITUDES (mag)	
		2004 Aug 28	2005 Apr 26
2M 1207			
F090M.....	0.80–1.00	14.66 $\pm$ 0.03	14.71 $\pm$ 0.04
F110M.....	1.00–1.20	13.44 $\pm$ 0.03	...
F145M.....	1.35–1.55	...	13.09 $\pm$ 0.03
F160W.....	1.40–1.80	12.60 $\pm$ 0.03	12.63 $\pm$ 0.02
2M 1207b			
F090M.....	0.80–1.00	22.34 $\pm$ 0.35	22.58 $\pm$ 0.35
F110M.....	1.00–1.20	20.61 $\pm$ 0.15	...
F145M.....	1.35–1.55	...	19.05 $\pm$ 0.03
F160W.....	1.40–1.80	18.24 $\pm$ 0.02	18.27 $\pm$ 0.02

NOTES.—The uncertainties in the NICMOS magnitudes include error estimates from the model PSF fitting (companion) and aperture photometry (primary), as well as the uncertainties in the absolute photometric calibration of the instrument in each filter band for camera 1. Chauvin et al. (2004) reported *JHKL'* photometry of 2M 1207 (*J* = 13.00  $\pm$  0.03 mag, *H* = 12.39  $\pm$  0.03 mag, *K* = 11.95  $\pm$  0.03 mag, and *L'* = 11.38  $\pm$  0.10 mag) and 2M 1207b (*H* = 18.09  $\pm$  0.21 mag, *K* = 16.93  $\pm$  0.11 mag, and *L'* = 15.28  $\pm$  0.14 mag). The NICMOS F160W filter is  $\sim$ 30% wider than the ground-based Johnson *H*-band filters, so comparison of our data with previously published *H*-band data requires a careful conversion (see Lowrance et al. 2000 for details).

count-rate images were geometrically corrected to yield flux-conserved resampled pixels of 43.190 mas pixel<sup>-1</sup> in both axes. All astrometric measures were made on the geometrically corrected images.

The location of the primary was measured from the combined image by Gaussian profile fitting of the primary's PSF core. We also measured the position of a serendipitously appearing field star, which could be used for future epoch differential proper motion measures of 2M 1207 itself (Table 3).

The locations of the companion, one from each field orientation at each epoch, were determined by the position offsets of

the model PSF implants used to null the companion images. The relative positions of 2M 1207 and its companion were transformed to position angle (P.A.; degrees east of north) and angular separation (in milliarcseconds) based on the well-established *HST* NICMOS focal plane metrology (aperture orientation in the telescope focal plane), the celestial orientation of the spacecraft, and the detector *X/Y* image scales of NICMOS camera 1.

### 3. 2M 1207 COLOR INDICES AND IMPLICATIONS

In Figure 2 (*left*),  $m_{\text{F090M}} - m_{\text{F160W}}$  and  $m_K - m_L$  colors of 2M 1207 and 2M 1207b (Table 2) are compared to those of model calculations—the “dusty model” (Chabrier et al. 2000) and “clear model” (Baraffe et al. 2003)—and field M, L, and T dwarfs from Leggett et al. (2002). Our red colors are consistent with Chauvin et al. (2004), who noted that 2M 1207b has a very red color ( $m_H - m_K = 1.16$  mag) even compared to most known L dwarfs. Our colors for 2M 1207b fall between two extreme model cases indicating that dust clouds significantly affect its atmosphere. AB Pic b, a  $\sim$ 13 Jupiter mass ( $M_J$ ) young planetary (or brown dwarf) companion to the  $\sim$ 30 Myr old K2 V star AB Pic (Chauvin et al. 2005b), also has unusually red near-IR colors for an L1 dwarf (Fig. 2, *right*). A field L dwarf, 2MASS J01415823–4633574, with very low surface gravity also shows very red near-IR colors (Kirkpatrick et al. 2006). In each of these cases, the unusual redness of these objects must be related to low surface gravity due to youth, and this extreme red color can be used to identify young brown dwarfs in the solar neighborhood.

With our estimated distance of 59  $\pm$  7 pc (see § 5), F090M and F160W absolute magnitudes imply a mass of  $2M_J$ – $8M_J$  for 2M 1207b (“dusty” model:  $5M_J$ – $8M_J$ ; “clear” model:  $2M_J$ – $5M_J$ ). On the other hand, the best estimated mass of 2M 1207b from a color-color diagram (Fig. 2, *left*) is  $6M_J$ – $8M_J$ . From these mass ranges, the mass of 2M 1207b is estimated to be  $5M_J \pm 3M_J$ , and the temperature corresponding to this mass range is 920–1540 K. Our estimated mass is consistent with the earlier estimate by Chauvin et al. (2004) from *HKL'* photometric data ( $5M_J \pm 2M_J$ ), which was based on a larger distance (70 pc). The fact that we derive the same estimated mass with a smaller distance indicates that 2M 1207b is brighter at shorter wavelengths

TABLE 3  
DIFFERENTIAL ASTROMETRY OF 2M 1207b RELATIVE TO 2M 1207

Epoch (UT)	Separation (mas)	Position Angle (deg E of N)	Instrument and Camera
2M 1207b			
2004 Apr 27.....	772 $\pm$ 4	125.4 $\pm$ 0.3	VLT NACO
2004 Aug 28.....	773.7 $\pm$ 2.2	125.37 $\pm$ 0.03	<i>HST</i> NICMOS
2005 Feb 05.....	768 $\pm$ 5	125.4 $\pm$ 0.3	VLT NACO
2005 Mar 31.....	776 $\pm$ 8	125.5 $\pm$ 0.3	VLT NACO
2005 Apr 26.....	773.5 $\pm$ 2.3	125.61 $\pm$ 0.20	<i>HST</i> NICMOS
Weighted mean ( <i>HST</i> + VLT)	773.0 $\pm$ 1.4	125.37 $\pm$ 0.03	...
Field Star			
2004 Aug 28.....	7795.3 $\pm$ 3.1	125.33 $\pm$ 0.01	...
2005 Apr 26.....	7848.9 $\pm$ 3.4	125.08 $\pm$ 0.06	...

NOTES.—The uncertainties in the *HST* position measurements include known calibration errors in the NICMOS science instrument aperture frame, image centroiding, and the absolute error in the spacecraft orientation as determined from ancillary engineering telemetry downlinked from the *HST* pointing control system. Listed positions are for the F160W image centroids, which are favored over other bands because (1) they were identically observed in this highest S/N bandpass at both epochs and (2) F160W PSFs ( $\lambda/D \sim 0''.14$ ) are better sampled with the camera 1 pixel scale (43 mas pixel<sup>-1</sup>) than the shorter wavelength observations. Positions were measured in all filter bands, and while all are consistent within their errors, the others are not quite as well determined as those made with F160W.

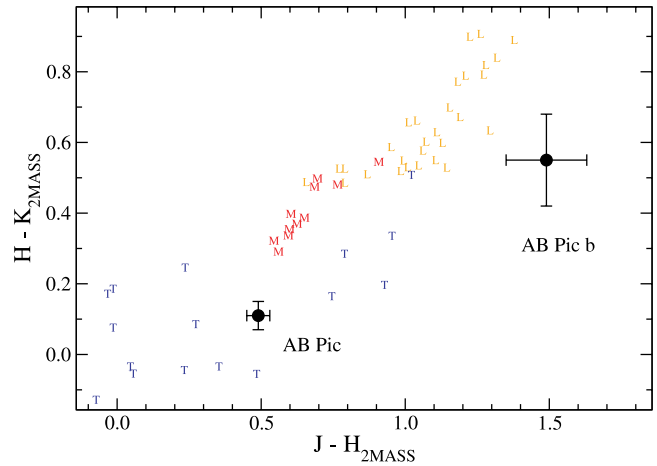
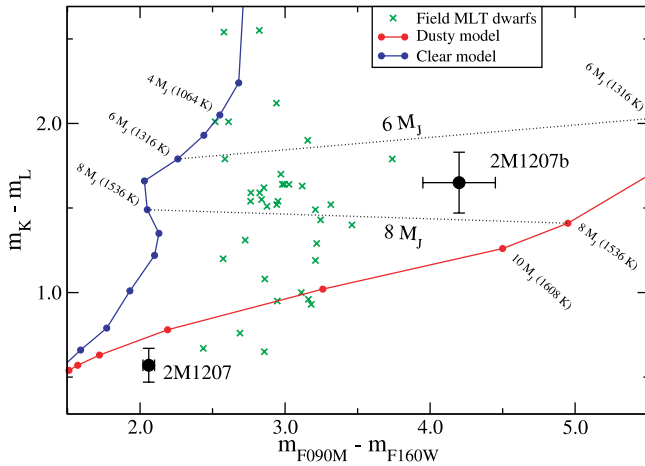


FIG. 2.—*Left*: NICMOS (from this study) and broadband (from Chauvin et al. 2004) colors of 2M 1207 and 2M 1207b compared to “dusty” (Chabrier et al. 2000) and “clear” (Baraffe et al. 2003) models. F090M and F160W magnitudes of field M, L, and T dwarfs (Leggett et al. 2002) are calculated using the IRAF task `synphot` from their measured ground-based spectra. *Right*: Near-IR colors of AB Pic and AB Pic b (Chauvin et al. 2005b) compared to those of field M, L, and T dwarfs (Leggett et al. 2002). For both 2M 1207b (L5 or later) and AB Pic b (L1), their extreme red color is caused by low surface gravity, which is in turn attributed to their young ages. Fig. 3 from Chauvin et al. (2004) shows a similar redness of 2M 1207b in  $HKL'$  colors.

(e.g., F090M) than model predictions, which implies a bluer  $m_{F090M} - m_{F160W}$  color than expected. Unusually red  $m_H - m_K$  and blue  $m_{F090M} - m_{F160W}$  colors could indicate that 2M 1207b is somewhat subluminescent in the  $H$  (F160W) band compared to models and to field L dwarfs.

#### 4. CONFIRMATION OF PHYSICAL COMPANIONSHIP

##### 4.1. Improved Proper-Motion Determination of 2M 1207

Scholz et al. (2005) estimated the proper motion<sup>7</sup> of 2M 1207 as  $(\mu_\alpha, \mu_\delta) = (-78 \pm 11, -24 \pm 9)$  mas yr<sup>-1</sup>, using positions from the SuperCOSMOS, Two Micron All Sky Survey (2MASS), and Deep Near Infrared Survey of the Southern Sky (DENIS) catalogs and from the *Chandra X-Ray Observatory* database. As there are large differences in the accuracy between the SuperCOSMOS, 2MASS, and DENIS positions (e.g., <60 mas for 2MASS vs. <500 mas for SuperCOSMOS), a precise and reliable estimate of proper motion was difficult to obtain (Mamajek 2005). Mamajek (2005) estimated proper motions of 2M 1207  $(\mu_\alpha, \mu_\delta) = (-72 \pm 7, -22 \pm 9)$  mas yr<sup>-1</sup> using positions from the same set of catalogs as in Scholz et al. (2005) excepting the problematic *Chandra* pointing position. Mamajek’s calculation takes into account the positional errors of input catalog positions, and his derived proper motions are overlapping, within errors, with our proper-motion measurements described below. However, as discussed in § 5, there are some caveats with respect to the analysis by Mamajek (2005).

A more precise measurement of 2M 1207’s proper motion was obtained in the following manner. On 2005 March 2, a single 120 s exposure  $I_C$ -band image of the field surrounding 2M 1207 was obtained at a parallactic angle of 44°.15 using the Tektronix 2048 × 2048 CCD camera on the University of Hawaii 2.2 m

telescope at Mauna Kea Observatory. The measured FWHM of point sources in the frame was 1".1 (5 pixels). An archival image, observed on 1978 May 2, was retrieved from the SuperCOSMOS Sky Survey database, for which a digitized scan was extracted from a UK Schmidt telescope plate. Because the  $I_C$ -band frame was obtained through high air mass (3.3) and because 2M 1207 is considerably redder than other objects in the frame, differential atmospheric refraction could affect the estimated proper motions (Monet et al. 1992). The IRAF task `synphot` was used to calculate the shift in effective wavelength between a typical field star (average G8) and 2M 1207 (M8), resulting in a 175 Å shift in the Cousins  $I$ -band filter. At the observed elevation of 17°.7, this shift from 7890 to 8065 Å yields a differential refraction of ≈50 mas (Howell 2000), which is small compared to the centroid shift of ∼1800 mas over 27 yr. Moreover, Howell’s calculation is for an altitude of 2.2 km, whereas our measurement was done at an altitude of 4.1 km; thus, the true differential atmospheric refraction effect should be smaller than 50 mas.

About 60 point sources were selected within the common 7'.5 × 7'.5 field of view of the  $I_C$ -band image and the 1978.33 SuperCOSMOS image. These point sources have centroids that are measured with robust S/N (≥10, unsaturated) and without obvious proper motion when blinking with the 2005  $I_C$ -band image. The centroid coordinates of the sources together with those of 2M 1207 were entered into the IRAF routine `geomap`, which calculates a general coordinate transformation, including rotation and distortion. The deviation (while excluded from the calculation) of 2M 1207 from the resulting coordinate transformation should be its relative motion with respect to the field sources, whose residuals give a measurement of the standard error. The resulting proper motion of 2M 1207 is calculated to be  $\mu_\alpha = -60.2 \pm 4.9$  mas yr<sup>-1</sup> and  $\mu_\delta = -25.0 \pm 4.9$  mas yr<sup>-1</sup>.

In order to assess the proper motion of 2M 1207 without the effects of differential atmospheric refraction, another  $I$ -band image was obtained on 2006 July 8 (2006.52) at the Siding Spring Observatory 1 m telescope using the Wide Field Imager. A 480 s exposure was taken at air mass 1.06 (elevation 71°) with measured point source FWHMs of 1".5 (4 pixels). At this elevation, there should be negligible differential atmospheric refraction. Using the method described above against the 1978.33 epoch SuperCOSMOS image with 62 point sources in common, we

<sup>7</sup> We note that two notations are used in the literature for proper motions in the R.A. direction:  $\mu_\alpha$  and  $\mu_\alpha \cos \delta$ . While it is true that the number of arcseconds to go once around in R.A. changes as a function of declination (so the need of the  $\cos \delta$  term), nothing else changes. Offsets, proper motions, etc., given in arcseconds are not dependent on declination. Therefore, it is not necessary or even correct to use the notation  $\mu_\alpha \cos \delta$  for proper motions given in arcseconds per year as in *Hipparcos*, *Tycho-2*, *UCAC2*, etc. Here we follow precedent as established by Gliese (1969) in his *Catalog of Nearby Stars* and list proper motions in arcseconds per year.

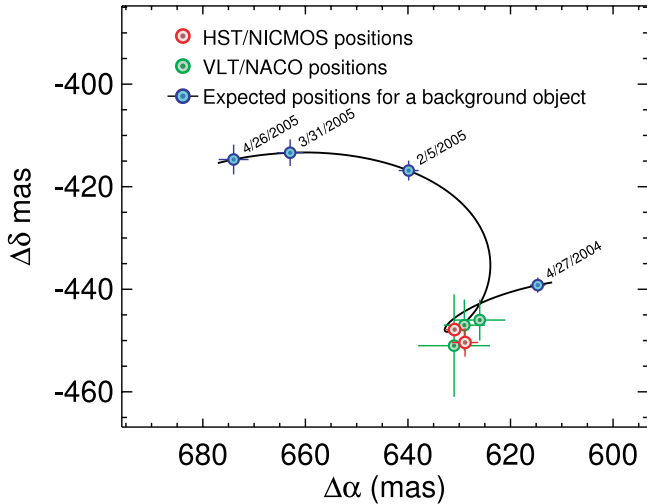


Fig. 3.—Unchanging separation and position angle between 2M 1207 and 2M 1207b. Observations with the *HST* and VLT prove that 2M 1207 and its planetary-mass companion share common proper motion, which means they are gravitationally bound. The green and red crosses mark the observed positions of the companion relative to 2M 1207 on different dates. Were the planetary-mass candidate seen in the 2004 August 28 image a stationary background object, then its position, relative to the position measured on 2004 August 28, would have changed as shown by the black line. A distance of 59 pc was used to calculate expected background positions.

calculate  $\mu_\alpha = -61.0 \pm 4.6$  mas yr<sup>-1</sup> and  $\mu_\delta = -20.1 \pm 4.9$  mas yr<sup>-1</sup>, which is in good agreement with the analysis above.

A final proper-motion value is estimated from the weighted average of the 1978/2005 and 1978/2006 epoch values:  $\mu_\alpha = -60.6 \pm 3.4$  mas yr<sup>-1</sup> and  $\mu_\delta = -22.6 \pm 3.5$  mas yr<sup>-1</sup>. The listed errors at each epoch are the scatter in field sources produced by geomap. For a distance of 59 pc, the annual parallax of 2M 1207 of 17 mas has negligible effect on our calculation because the 1978/2005/2006 measurements were obtained during similar seasons of the year. Furthermore, even for the worst case (17 mas offset for the 27 yr baseline), this effect is much less than the random centroiding error.

#### 4.2. Common Proper Motion Pair

Measured separations between 2M 1207 and 2M 1207b from the *HST* and VLT are listed in Table 3. Due to the proper motion of the primary, relative positions between the primary and a stationary background object should change over time as illustrated in Figure 3. Because the 2004 August 28 *HST* observation has the best positional measurement accuracy, all other positions are plotted relative to it. If the planetary-mass companion candidate seen in the 2004 August 28 image had been a stationary background source, then its position relative to 2M 1207 would have changed along the black line of Figure 3. As clearly shown in Figure 3 and Table 3, 2M 1207 and its planetary-mass companion (2M 1207b) are comoving, indicative of a gravitationally bound pair.

The weighted mean offset position of 2M 1207b relative to 2M 1207 from *HST* and VLT images is  $\Delta\alpha = 629.8 \pm 1.3$  mas and  $\Delta\delta = -448.1 \pm 1.1$  mas. Comparing this against the expected position for a background object at epoch 2005 April 26,  $\Delta\alpha = 674.6 \pm 2.2$  mas and  $\Delta\delta = -415.6 \pm 2.3$  mas, we find that the two positions differ by 16.2  $\sigma$ . Using only the *HST* images, the level drops to 16.0  $\sigma$ , which is an unambiguous independent confirmation of the proper-motion companionship of 2M 1207 and 2M 1207b. Uncertainties in background object po-

sition were calculated using our improved proper motions and distance (59 pc; see § 5 for details on distance estimation).

## 5. DISCUSSION

Chauvin et al. (2005a) argue that the mass of 2M 1207b falls in the planetary range ( $< 13.6M_J$ ). To prove this conjecture one must establish that (1) 2M 1207 is very young, i.e., a member of the  $\sim 8$  Myr old TW Hydrae association (TWA), and (2) 2M 1207 and 2M 1207b are gravitationally bound.

Provided that conditions 1 and 2 are true, then Chauvin et al. (2004, 2005a) describe how two essentially independent techniques—evolutionary modeling and surface gravity analysis—both yield masses for 2M 1207b well below  $13.6M_J$ . In Figure 3 and Table 3 of the present paper, we establish with high confidence that 2M 1207 and 2M 1207b are gravitationally bound.

Thus, only membership of 2M 1207 in the TWA remains to be considered. Chauvin et al. (2004) list a variety of reasons (their § 3.1) why 2M 1207 is a member of the TWA. We can now strengthen their argument. Ongoing Keck NIRSPEC spectroscopic surveys of brown dwarfs, both old and young, (e.g., McGovern 2005; McGovern et al. 2004; McLean et al. 2003), corroborate earlier measurements (mentioned in Chauvin et al. 2004) indicating low surface gravity in 2M 1207, characteristic of a  $\sim 10$  Myr brown dwarf. Mohanty et al. (2005) report a detection of [O I] emission, which indicates a mass outflow from 2M 1207, as well as a detection of accretion shock-induced UV emission (see their § 5.1 for details). All these strongly support that 2M 1207 is indeed a young accreting brown dwarf.

Using our new determination of the proper motion of 2M 1207, we can derive a more reliable estimate of the distance to 2M 1207 than was available to Chauvin et al. TWA members HR 4796A and 2M 1207 lie very close together in the plane of the sky and thus should have proper motions that differ only according to their relative distances from Earth. The proper motion of HR 4796A is given in the Tycho-2 catalog ( $\mu_\alpha = -53.3 \pm 1.3$  mas yr<sup>-1</sup>,  $\mu_\delta = -21.2 \pm 1.1$  mas yr<sup>-1</sup>). We used Tycho-2 proper motions over published, ostensibly more precise, *Hipparcos* values because *Hipparcos* proper-motion uncertainties seem to have been underestimated (e.g., Kaplan & Snell 2001; Soderblom et al. 2005). From the ratio of total proper motions of HR 4796A and 2M 1207 (1.144:1.000) and using the *Hipparcos* measured distance to HR 4796A ( $67.1 \pm 3.4$  pc), we deduce a distance to 2M 1207 of  $59 \pm 7$  pc. At this distance, the projected separation of 2M 1207b from 2M 1207 is  $46 \pm 5$  AU.

Our proper-motion-based method to derive the distance to 2M 1207 can be tested on TWA 25, which is also close in the plane of the sky to HR 4796A. The proper motion of TWA 25 is  $(-75.9, -26.3)$ ; thus, from the ratio of total proper motion to HR 4796A (1.400:1.000), one derives a distance to TWA 25 of  $\sim 48$  pc. This is in good agreement with the photometric distance of 44 pc given in Song et al. (2003). In this case (unlike 2M 1207), because TWA 25 is an M0 dwarf and there are many similar spectral type members in the TWA, the photometric distance should be fairly reliable. Thus, the agreement between the proper motion and photometrically derived distances for TWA 25 supports the proper-motion method we use to derive the distance to 2M 1207.

Using the moving cluster method, Mamajek (2005) estimated a somewhat smaller distance ( $53 \pm 6$  pc) to 2M 1207. Because the moving cluster method to the TWA is grounded in good *Hipparcos* measured distances to only three stars (TW Hya, HD 98800, and HR 4796A; the *Hipparcos* distance to TWA 9 appears to be wrong), conclusions drawn in the study of Mamajek (2005) should be regarded with care. For example, that study rejects TWA membership for the nearby ( $\sim 22$  pc) mid-M dwarf TWA 22

(Song et al. 2003) because doing so substantially improves the vertex solution presented. Yet TWA 22 has a very strong lithium line (Song et al. 2003), and our survey of nearby, active, M-type stars over most of the sky (I. Song, M. Bessell, & B. Zuckerman, 2006, in preparation) has revealed strong lithium lines only in the direction of the TWA with the exception of a very few M-type members of the  $\beta$  Pic moving group. However, as the  $\beta$  Pic moving group has nearly the same Galactic space motion as the TWA (Zuckerman & Song 2004, Table 7), even in the very unlikely event that TWA 22 is a  $\beta$  Pic member, this could hardly impact the vertex solution. In addition, TWA 22 turns out to be a  $\sim 0''.1$  binary with  $\Delta K \sim 0.4$  mag (G. Chauvin et al. 2006, in preparation), pushing its photometric distance from 22 to 28 pc. Therefore, TWA 22 is very likely a true TWA member. Because of such issues, we adopt our  $59 \pm 7$  pc distance determination for 2M 1207, in preference to earlier estimates.

Calculations of opacity-limited fragmentation in a turbulent three-dimensional medium yield minimum masses  $\geq 7M_J$  (e.g., Low & Lynden-Bell 1976; Boyd & Whitworth 2005; Bate 2005 and references therein). Given the uncertainties in these calculations and in evolutionary models of young, planetary-mass objects, our  $5M_J \pm 3M_J$  estimate for 2M 1207b is likely not in conflict with the  $7M_J$  fragmentation mass. Alternatively, perhaps a different model, for example, two-dimensional fragmentation of a shock-compressed layer (Boyd & Whitworth 2005), would ultimately be needed to account for the properties of 2M 1207b.

## 6. CONCLUSIONS

The common proper motion confirmation of the first imaged planetary-mass companion to a celestial object other than our Sun enables the onset of a new era in extrasolar planet characterization: direct spectroscopic analysis. Absorption spectroscopy of

stellar light reprocessed through atmospheres of planets detected through radial velocity surveys has been demonstrated (e.g., HD 209458b; Brown et al. 2001). 2M 1207b provides the first opportunity to collect and spectroscopically analyze photons from an extrasolar planetary-mass companion. By exploiting the superb stability of the *HST*, we will attempt to obtain a near-IR grism spectrum of 2M 1207b. Relative to clear atmospheric models, dusty models (e.g., Chabrier et al. 2000) predict more flux suppression in the 1.0–1.3  $\mu\text{m}$  range, which can be readily compared to the anticipated S/N  $\sim 10$  grism spectrum.

This research was supported by STScI through grant HST-GO-10176. Portions of this research were performed under the auspices of the US Department of Energy by the University of California, Lawrence Livermore National Laboratory under contract W-7405-ENG-48. We thank Michael Wenz (STScI) and Merle Reinhart (CSC) for their assistance in determining *HST*'s absolute orientation error following the guide star acquisitions for each of our orbits. Our gratitude is extended to Al Schultz and Beth Perrillo (our contact scientist and program coordinator at STScI) for their assistance in implementing and scheduling our observations. We thank Richard Crowe for kindly obtaining the 2005 *I*-band data and Bob Shobbrook for the 2006 *I*-band image used in our proper-motion refinement. We thank the referee for pointing out to us the potential importance of differential atmospheric refraction in our 2005 *I*-band image. This work was supported by the Gemini Observatory, which is operated by the Association of Universities for Research in Astronomy, Inc., on behalf of the international Gemini partnership of Argentina, Australia, Brazil, Canada, Chile, the United Kingdom, and the United States of America.

## REFERENCES

- Baraffe, I., Chabrier, G., Barman, T. S., Allard, F., & Hauschildt, P. H. 2003, *A&A*, 402, 701  
 Bate, M. R. 2005, *MNRAS*, 363, 363  
 Boyd, D. F. A., & Whitworth, A. P. 2005, *A&A*, 430, 1059  
 Brown, T. M., Charbonneau, D., Gilliland, R. L., Noyes, R. W., & Burrows, A. 2001, *ApJ*, 552, 699  
 Chabrier, G., Baraffe, I., Allard, F., & Hauschildt, P. 2000, *ApJ*, 542, 464  
 Chauvin, G., et al. 2004, *A&A*, 425, L29  
 ———. 2005a, *A&A*, 438, L25  
 ———. 2005b, *A&A*, 438, L29  
 Gizis, J. E. 2002, *ApJ*, 575, 484  
 Gliese, W. 1969, *Veröff. Astron. Rech.-Inst. Heidelberg*, 22, 1  
 Howell, S. B. 2000, *Handbook of CCD Astronomy* (Cambridge: Cambridge Univ. Press)  
 Kaplan, G. H., & Snell, S. C. 2001, *BAAS*, 33, 1493  
 Kirkpatrick, J. D., Barman, T. S., Burgasser, A. J., McGovern, M. R., McLean, I. S., Tinney, C. G., & Lowrance, P. J. 2006, *ApJ*, 639, 1120  
 Krist, J. E., & Hook, R. N. 1997, in *The 1997 HST Calibration Workshop with a New Generation of Instruments*, ed. S. Casertano & C. Skinner (Baltimore: STScI), 192  
 Leggett, S. K., et al. 2002, *ApJ*, 564, 452  
 Low, C., & Lynden-Bell, D. 1976, *MNRAS*, 176, 367  
 Lowrance, P. J., et al. 2000, *ApJ*, 541, 390  
 Mamajek, E. E. 2005, *ApJ*, 634, 1385  
 McGovern, M. R. 2005, Ph.D. thesis, Univ. California, Los Angeles  
 McGovern, M. R., et al. 2004, *ApJ*, 600, 1020  
 McLean, I. S., McGovern, M. R., Burgasser, A. J., Kirkpatrick, J. D., Prato, L., & Kim, S. S. 2003, *ApJ*, 596, 561  
 Mohanty, S., Jayawardhana, R., & Basri, G. 2005, *ApJ*, 626, 498  
 Monet, D. G., Dahn, C. C., Vrba, F. J., Harris, H. C., Pier, J. R., Luginbuhl, C. B., & Ables, H. D. 1992, *AJ*, 103, 638  
 Noll, K., et al. 2004, *NICMOS Instrument Handbook*, Ver. 7 (Baltimore: STScI)  
 Schneider, G., Silverstone, M. D., & Hines, D. C. 2005, *ApJ*, 629, L117  
 Schneider, G., et al. 2004, *BAAS*, 36, 1354  
 Scholz, R.-D., McCaughrean, M. J., Zinnecker, H., & Lodieu, N. 2005, *A&A*, 430, L49  
 Soderblom, D. R., Nelan, E., Benedict, G. F., McArthur, B., Ramirez, I., Spiesman, W., & Jones, B. F. 2005, *AJ*, 129, 1616  
 Song, I., Zuckerman, B., & Bessell, M. S. 2003, *ApJ*, 599, 342  
 Zuckerman, B., & Song, I. 2004, *ARA&A*, 42, 685